Smart Structures and Systems, *Vol. 24, No. 6 (2019) 683-692*
DOI: https://doi.org/10.12989/sss.2019.24.6.683

Nonlinear finite element model updating with a decentralized approach

P.H. Ni[1a] and X.W. Ye[*2]

[1]*Key Laboratory of Urban Security and Disaster Engineering of Ministry of Education, Beijing University of Technology, Beijing 100124, China*
[2]*Department of Civil Engineering, Zhejiang University, Hangzhou 310058, China*

(Received May 16, 2019, Revised July 26, 2019, Accepted August 1, 2019)

Abstract. Traditional damage detection methods for nonlinear structures are often based on simplified models, such as the mass-spring-damper and shear-building models, which are insufficient for predicting the vibration responses of a real structure. Conventional global nonlinear finite element model updating methods are computationally intensive and time consuming. Thus, they cannot be applied to practical structures. A decentralized approach for identifying the nonlinear material parameters is proposed in this study. With this technique, a structure is divided into several small zones on the basis of its structural configuration. The unknown material parameters and measured vibration responses are then divided into several subsets accordingly. The structural parameters of each subset are then updated using the vibration responses of the subset with the Newton-successive-over-relaxation (SOR) method. A reinforced concrete and steel frame structure subjected to earthquake loading is used to verify the effectiveness and accuracy of the proposed method. The parameters in the material constitutive model, such as compressive strength, initial tangent stiffness and yielding stress, are identified accurately and efficiently compared with the global nonlinear model updating approach.

Keywords: nonlinear finite element method; model updating; system identification; decentralized approach

1. Introduction

System identification methods for identifying structural damage in the early stage have gained attention since the 1990s (Friswell and Mottershead 2013). Numerous techniques have since been developed (Ye *et al.* 2013, Ni *et al.* 2014, Ye *et al.* 2016a, b). However, the majority of these methods assume that structural behaviors remain in the linear elastic stage after damage has occurred. This assumption may be incorrect because damage generally causes a structure in the nonlinear state. For example, a strong earthquake may cause cracks in a structure; the opening and closing of cracks exhibit a nonlinear property (Chen *et al*. 2006, Prawin *et al*. 2018). Therefore, nonlinear structural behaviors should be considered in damage identification.

The nonlinear characteristics of structures have been identified using Bayesian approach (Yuen and Beck 2003), least squares algorithm (Smyth *et al*. 1999), Kalman filter (Chatzi and Smyth 2009) and intelligence algorithm (Charalampakis and Koumousis 2008). For example, Yuen and Beck (2003) proposed a nonlinear parameter identification method based on a spectral density. A stochastic model was used to represent the uncertainty of a random input, whereas a Bayesian probabilistic approach was developed to quantify the parameters in the stochastic model. Ting *et al*. (2006) developed a Bayesian technique to estimate the parameters in a rigid body dynamics system. The Bayesian regularization method was applied to ensure the robustness of the algorithm by considering the noise in the measured responses and input force. Xu *et al*. (2012) proposed a power series polynomial model to represent the nonlinear restoring force. The least squares technique was developed to estimate the coefficients of the polynomial model. The proposed method was applied to a nonlinear multiple degree-of-freedom (DOF) chain-like structure without prior knowledge of the system model. The nonlinear restoring force and unknown dynamic loadings were successfully identified. An experimental study on a four-storey steel frame structure equipped with two actively controlled magnetorheological dampers was also conducted (He *et al*. 2012). Lei and Wu (2011) developed a technique to identify the nonlinear restoring force with limited input and output measurements. The unknown system parameters were identified by using a two-stage Kalman estimator technique with vibration responses. The nonlinear restoring force and unmeasured excitation were estimated using the recursive least squares method.

The majority of these existing studies use simplified models to calculate the nonlinear vibration responses of structures. These models, including the mass-spring-damper and shear-building models, are based on simplified assumptions and are insufficient for predicting the vibration characteristics/responses of real structures. The recent development of nonlinear finite element (FE) methods, particularly with improvements in computer efficiency and capability, enables the simulation of the complex nonlinear behaviours of large-scale structures under earthquake inputs. Existing nonlinear FE methods have focused on

*Corresponding author, Ph.D., Professor
E-mail: cexwye@zju.edu.cn
[a] Assistant Professor

Copyright © 2019 Techno-Press, Ltd.
http://www.techno-press.com/journals/sss&subpage=7
ISSN: 1738-1584 (Print), 1738-1991 (Online)

dynamic analysis (Taucer *et al*. 1991), seismic design and reliability evaluation (Haukaas and Der Kiureghian 2004). These studies have shown that the nonlinear FE methods can predict and model the nonlinear dynamic behaviour of structures with high accuracy.

Recently, nonlinear FE model updating has been developed to identify structural nonlinear parameters. Ebrahimian *et al*. (2015) utilised the extended Kalman filter to identify the material parameters in the constitutive models of reinforcement and concrete. Astroza *et al.* (2014) adopted the stochastic filtering technique to estimate the material parameters in the distributed plasticity of the FE model. Similar studies on nonlinear material parameter identification were conducted using the batch Bayesian approach (Ebrahimian *et al.* 2017). The unknown material parameter and seismic input were identified using the recursive Bayesian estimation approach (Astroza *et al.* 2017) and sequential maximum likelihood estimation algorithm (Ebrahimian *et al*. 2018). Experimental studies on nonlinear FE model updating were also conducted. Asgarieh *et al*. (2014) calibrated the nonlinear FE model of a masonry infilled frame structure. The parameters in the hysteretic material models were updated with time-varying modal parameters of the real structure. Li *et al*. (2017) performed an experimental investigation on a seismic isolated bridge. The parameters of the isolators were calibrated from the experimental test data, and the updated bridge model was consistent with the measured responses.

These nonlinear FE model updating methods are global based, that is, the unknown parameters of the entire structure are updated simultaneously. The nonlinear analysis is computationally intensive and time consuming; thus, the global approach cannot be applied to practical structures that contain a great number of DOFs. This study proposes a decentralized approach for nonlinear FE model updating. The dynamic responses of the structure are computed on the basis of the discrete FE models with nonlinear dynamic analysis. The nonlinear behavior of a structure is simulated using the uniaxial material model (Taucer *et al*. 1991). Following previous studies (Law *et al*. 2014, Ni *et al*. 2018), a large-scale structure is divided into several small zones on the basis of its FE configuration. Each subset of unknown material parameters is updated using the measured vibration responses at its own zone with the Newton-SOR method. The proposed method is implemented in MATLAB and interfaced with OpenSees (McKenna 2011) for calculating the dynamic responses and response sensitivity. Numerical studies on two building structures under ground motion inputs are conducted to verify the accuracy of the proposed method. Different material parameters in the constitutive parameters, such as the compressive strength of concrete and the yield stress of reinforcement, are regarded as unknown variables to be updated. Results show that the proposed decentralized method can accurately identify the nonlinear material parameters. The efficiency of the present method is also compared with that of the conventional global model updating approach.

2. Decentralized model updating approach

2.1 Nonlinear FE analysis procedure

The equation of motion of an N-DOFs damped nonlinear system under ground motion excitation can be written as follows

$$\boldsymbol{M}\ddot{\boldsymbol{x}}(t)+\boldsymbol{C}\dot{\boldsymbol{x}}(t)+\boldsymbol{K}_r\left(\boldsymbol{x}(t),\boldsymbol{\theta}\right)=\boldsymbol{MI}\ddot{x}_g(t) \tag{1}$$

where $\boldsymbol{x}(t)$, $\dot{\boldsymbol{x}}(t)$ and $\ddot{\boldsymbol{x}}(t)$ are the vectors of the displacements, velocity and acceleration responses of the structure at time t, respectively; $\boldsymbol{M}$ and $\boldsymbol{C}$ denote the mass and damping matrices of the structure, respectively; $\boldsymbol{\theta}$ is the material parameter vector in the material constitutive model; $\boldsymbol{K}_r\left(\boldsymbol{x}(t),\boldsymbol{\theta}\right)$ represents the resisting force vector and depends on $\boldsymbol{x}(t)$ and $\boldsymbol{\theta}$; and $\ddot{x}_g(t)$ refers to the ground motion acceleration. The mass matrix of a structure can be estimated accurately from the geometric dimension and material density, which are assumed invariant.

The fiber beam-column elements (Taucer *et al*. 1991) are used in this study for the nonlinear dynamic analysis of frame structures under seismic input. The structural model is initially divided into a number of elements. Then, the section of each element is discretized into several fibers, which follows a specific constitutive law of the material. Fig. 1 shows the computational model of the nonlinear dynamic analysis. The nonlinear analysis procedure contains state determination at the element, section and fiber levels. The fiber strain is computed from the section/element deformation with the plane section assumption. The stress and tangent moduli of each fiber are obtained from the material constitutive models with the fiber strain. Meanwhile, the section resisting forces are calculated by adding the axial force and biaxial bending moment contributions of all fibers. Finally, the element flexibility matrix is formed by integrating the section flexibility and then inverted to the element tangent stiffness matrix. Detailed descriptions of the technique are provided in previous study (Taucer *et al*. 1991).

2.2 Decentralized identification of nonlinear material parameters

Decentralized methods, as a promising solution in large structural health monitoring (SHM) systems, have been developed for modal identification (Kim and Lynch 2011), vibration control (Xu *et al*. 2003, Lei *et al*. 2013) and damage detection (Law *et al*. 2014, Ni *et al*. 2018) in large-scale structures. A decentralized approach for nonlinear FE model updating is developed in this study.

A large-scale system can be divided into several subsystems. Measurements in the structure are divided into small physical zones on the basis of its FE formulation. The unknown structural parameter $\boldsymbol{\theta}$ can be divided into r subsets $\left[\boldsymbol{\theta}_1,\ \boldsymbol{\theta}_2,\ \cdots,\ \boldsymbol{\theta}_r\right]$, where $\boldsymbol{\theta}_i$ contains all unknown material parameters of the ith ($1\le i\le r$) zone. Field testing is conducted in different zones of the structure. The measured dynamic responses from the ith zone $\ddot{\boldsymbol{x}}_{mea,i}$ can be written as a function as $\boldsymbol{g}_i(\boldsymbol{\theta}_1,\boldsymbol{\theta}_2,\cdots,\boldsymbol{\theta}_r,\ddot{x}_g)$. The measured responses from different zones can be expressed as

$$\begin{aligned} &\boldsymbol{g}_1(\boldsymbol{\theta}_1,\boldsymbol{\theta}_2,\cdots,\boldsymbol{\theta}_r,\ddot{x}_g)-\ddot{\boldsymbol{x}}_{mea,1}=0\\ &\boldsymbol{g}_2(\boldsymbol{\theta}_1,\boldsymbol{\theta}_2,\cdots,\boldsymbol{\theta}_r,\ddot{x}_g)-\ddot{\boldsymbol{x}}_{mea,2}=0\\ &\quad\vdots\qquad\vdots\\ &\boldsymbol{g}_i(\boldsymbol{\theta}_1,\boldsymbol{\theta}_2,\cdots,\boldsymbol{\theta}_r,\ddot{x}_g)-\ddot{\boldsymbol{x}}_{mea,i}=0\\ &\quad\vdots\qquad\vdots\\ &\boldsymbol{g}_r(\boldsymbol{\theta}_1,\boldsymbol{\theta}_2,\cdots,\boldsymbol{\theta}_r,\ddot{x}_g)-\ddot{\boldsymbol{x}}_{mea,r}=0 \end{aligned} \tag{2}$$

In Eq. (2), material parameters in the constitutive model are unknown and will be identified from a nonlinear FE model updating technique. Eq. (2) can be written as

$$\boldsymbol{G}(\boldsymbol{\theta})=0 \tag{3}$$

and solved using the Newton method (Ortega and Rheinboldt 1970) as follows

$$\boldsymbol{G}(\boldsymbol{\theta})=\boldsymbol{G}(\boldsymbol{\theta}^n)+\boldsymbol{G}'(\boldsymbol{\theta}^n)(\boldsymbol{\theta}^{n+1}-\boldsymbol{\theta}^n)=0 \tag{4}$$

$$\boldsymbol{G}'(\boldsymbol{\theta}^n)\boldsymbol{\theta}^{n+1}=\boldsymbol{G}'(\boldsymbol{\theta}^n)\boldsymbol{\theta}^n-\boldsymbol{G}(\boldsymbol{\theta}^n) \tag{5}$$

$$\boldsymbol{\theta}^{n+1}=\boldsymbol{\theta}^n-\left[\boldsymbol{G}'(\boldsymbol{\theta}^n)\right]^{-1}\boldsymbol{G}(\boldsymbol{\theta}^n) \tag{6}$$

where n denotes the number of iterations; and $\boldsymbol{G}'\left(\boldsymbol{\theta}^n\right)$ is the Jacobian matrix of $\boldsymbol{G}\left(\boldsymbol{\theta}^n\right)$ as

$$\boldsymbol{G}'(\boldsymbol{\theta}^n)=\begin{bmatrix} \frac{\partial\boldsymbol{g}_1}{\partial\boldsymbol{\theta}_1} & \frac{\partial\boldsymbol{g}_1}{\partial\boldsymbol{\theta}_2} & \cdots & \frac{\partial\boldsymbol{g}_1}{\partial\boldsymbol{\theta}_r}\\ \frac{\partial\boldsymbol{g}_2}{\partial\boldsymbol{\theta}_1} & \frac{\partial\boldsymbol{g}_2}{\partial\boldsymbol{\theta}_2} & \cdots & \frac{\partial\boldsymbol{g}_2}{\partial\boldsymbol{\theta}_r}\\ \vdots & \vdots & & \vdots\\ \frac{\partial\boldsymbol{g}_r}{\partial\boldsymbol{\theta}_1} & \frac{\partial\boldsymbol{g}_r}{\partial\boldsymbol{\theta}_2} & \cdots & \frac{\partial\boldsymbol{g}_r}{\partial\boldsymbol{\theta}_r} \end{bmatrix} \tag{7}$$

Following the derivation in previous study (Law *et al.* 2014), an iterative SOR method is applied to Eq. (5). The Jacobian matrix $\boldsymbol{G}'\left(\boldsymbol{\theta}^n\right)$ is decomposed into a diagonal block matrix $\boldsymbol{L}$ and non-diagonal block matrix $\boldsymbol{U}$ as follows

$$\boldsymbol{G}'\left(\boldsymbol{\theta}^n\right)=\boldsymbol{L}-\boldsymbol{U} \tag{8}$$

Eq. (5) can then be rewritten as follows

$$\left(\boldsymbol{L}-\boldsymbol{U}\right)\boldsymbol{\theta}^{n+1}=\boldsymbol{G}'\left(\boldsymbol{\theta}^n\right)\boldsymbol{\theta}^n-\boldsymbol{G}\left(\boldsymbol{\theta}^n\right) \tag{9}$$

The right-hand side of Eq. (9) is defined as follows

$$\boldsymbol{b}=\boldsymbol{G}'\left(\boldsymbol{\theta}^n\right)\boldsymbol{\theta}^n-\boldsymbol{G}\left(\boldsymbol{\theta}^n\right) \tag{10}$$

By substituting Eq. (10) into Eq. (9), we have

$$\boldsymbol{L}\boldsymbol{\theta}^{n+1}=\boldsymbol{U}\boldsymbol{\theta}^{n+1}+\boldsymbol{b} \tag{11}$$

By using the SOR method, Eq. (11) can be written as

$$\boldsymbol{L}\boldsymbol{\theta}^{n+1,q}=\boldsymbol{U}\boldsymbol{\theta}^{n+1,q-1}+\boldsymbol{b} \tag{12}$$

and

$$\boldsymbol{\theta}^{n+1,q}=\boldsymbol{L}^{-1}\left(\boldsymbol{U}\boldsymbol{\theta}^{n+1,q-1}+\boldsymbol{b}\right),\ (q=1,\ 2,\ 3,\cdots) \tag{13}$$

where superscript q denotes the iteration step in the SOR method.

By defining matrix $\boldsymbol{V}=\boldsymbol{L}^{-1}\boldsymbol{U}$, Eq. (13) can be rewritten as follows

$$\boldsymbol{\theta}^{n+1,q}=\boldsymbol{V}\boldsymbol{\theta}^{n+1,q-1}+\boldsymbol{L}^{-1}\boldsymbol{b} \tag{14}$$

By expanding $\boldsymbol{V}\boldsymbol{\theta}^{n+1,q-1}$, we have

$$\begin{aligned} \boldsymbol{\theta}^{n+1,q}&=\boldsymbol{V}^q\boldsymbol{\theta}^{n+1,0}+\left(\boldsymbol{I}+\boldsymbol{V}+\boldsymbol{V}^2\cdots\boldsymbol{V}^{q-1}\right)\boldsymbol{L}^{-1}\boldsymbol{b}\\ &=\boldsymbol{\theta}^{n+1,0}+\left(\boldsymbol{V}^q-\boldsymbol{I}\right)\boldsymbol{\theta}^{n+1,0}+\left(\boldsymbol{I}+\boldsymbol{V}+\boldsymbol{V}^2\cdots\boldsymbol{V}^{q-1}\right)\boldsymbol{L}^{-1}\boldsymbol{b}\\ &=\boldsymbol{\theta}^{n+1,0}+\left(\boldsymbol{I}+\boldsymbol{V}+\boldsymbol{V}^2\cdots\boldsymbol{V}^{q-1}\right)\left(\left(\boldsymbol{V}-\boldsymbol{I}\right)\boldsymbol{\theta}^{n+1,0}+\boldsymbol{L}^{-1}\boldsymbol{b}\right) \end{aligned} \tag{15}$$

Given

$$\boldsymbol{V}-\boldsymbol{I}=\boldsymbol{L}^{-1}\boldsymbol{U}-\boldsymbol{I}=\boldsymbol{L}^{-1}\left(\boldsymbol{U}-\boldsymbol{L}\right) \tag{16}$$

The last bracket on the right-hand side of Eq. (15) can be expressed as

$$\begin{aligned} &\left(\boldsymbol{V}-\boldsymbol{I}\right)\boldsymbol{\theta}^{n+1,0}+\boldsymbol{L}^{-1}\boldsymbol{b}\\ &=\boldsymbol{L}^{-1}\left(\boldsymbol{U}-\boldsymbol{L}\right)\boldsymbol{\theta}^{n+1,0}+\boldsymbol{L}^{-1}\left(\left(\boldsymbol{L}-\boldsymbol{U}\right)\boldsymbol{\theta}^n-\boldsymbol{G}\left(\boldsymbol{\theta}^n\right)\right)\\ &=\boldsymbol{L}^{-1}\left(\boldsymbol{U}-\boldsymbol{L}\right)\left(\boldsymbol{\theta}^{n+1,0}-\boldsymbol{\theta}^n\right)-\boldsymbol{L}^{-1}\boldsymbol{G}\left(\boldsymbol{\theta}^n\right) \end{aligned} \tag{17}$$

The initial and ending values of the SOR iteration are the initial and ending values of the Newton iteration, respectively: $\boldsymbol{\theta}^{n+1,0}\equiv\boldsymbol{\theta}^n$ and $\boldsymbol{\theta}^{n+1,q}\equiv\boldsymbol{\theta}^{n+1}$. By substituting Eq. (17) into Eq. (15), we have

$$\boldsymbol{\theta}^{n+1}=\boldsymbol{\theta}^n-\left(\boldsymbol{I}+\boldsymbol{V}+\boldsymbol{V}^2\cdots\boldsymbol{V}^{q-1}\right)\boldsymbol{L}^{-1}\boldsymbol{G}\left(\boldsymbol{\theta}^n\right) \tag{18}$$

When $q\to\infty$, Eq. (18) is equivalent to the Newton method in Eq. (6). When q=1, we have the one-step Newton-SOR iteration as follows

$$\boldsymbol{\theta}^{n+1}=\boldsymbol{\theta}^n-\boldsymbol{L}^{-1}\boldsymbol{G}\left(\boldsymbol{\theta}^n\right) \tag{19}$$

By rewriting $\boldsymbol{\theta}^{n+1}$ into a vector of subsets $\left[\boldsymbol{\theta}_1^{n+1},\ \boldsymbol{\theta}_2^{n+1},\cdots,\boldsymbol{\theta}_r^{n+1}\right]$, Eq. (19) can be expressed as

$$\boldsymbol{\theta}_i^{n+1}=\boldsymbol{\theta}_i^n-\left[\frac{\partial\boldsymbol{g}_i}{\partial\boldsymbol{\theta}_i^n}\right]^{-1}\left[\boldsymbol{g}_i\left(\boldsymbol{\theta}^n,\ \boldsymbol{f}_i\right)-\ddot{\boldsymbol{x}}_{mea,i}\right]\quad\left(i=1,2,\cdots,r\right) \tag{20}$$

or

$$\begin{bmatrix}\boldsymbol{\theta}_1^{n+1}\\ \boldsymbol{\theta}_2^{n+1}\\ \vdots\\ \boldsymbol{\theta}_r^{n+1}\end{bmatrix}=\begin{bmatrix}\boldsymbol{\theta}_1^{n}\\ \boldsymbol{\theta}_2^{n}\\ \vdots\\ \boldsymbol{\theta}_r^{n}\end{bmatrix}-\begin{bmatrix}\frac{\partial\boldsymbol{g}_1}{\partial\boldsymbol{\theta}_1^n} & 0 & 0 & 0\\ 0 & \frac{\partial\boldsymbol{g}_2}{\partial\boldsymbol{\theta}_2^n} & 0 & 0\\ 0 & 0 & \ddots & 0\\ 0 & 0 & 0 & \frac{\partial\boldsymbol{g}_r}{\partial\boldsymbol{\theta}_r^n}\end{bmatrix}^{-1}\begin{bmatrix}\boldsymbol{g}_1\left(\boldsymbol{\theta}^n,\ \boldsymbol{f}_1\right)-\ddot{\boldsymbol{x}}_{mea,1}\\ \boldsymbol{g}_2\left(\boldsymbol{\theta}^n,\ \boldsymbol{f}_2\right)-\ddot{\boldsymbol{x}}_{mea,2}\\ \vdots\\ \boldsymbol{g}_r\left(\boldsymbol{\theta}^n,\ \boldsymbol{f}_r\right)-\ddot{\boldsymbol{x}}_{mea,r}\end{bmatrix},\quad\left(i=1,2,\cdots,r\right) \tag{21}$$

The least squares method is applied to Eq. (20), and the resulting one-step Newton-SOR is obtained as follows

$$\boldsymbol{\theta}_i^{n+1} = \boldsymbol{\theta}_i^n - \left[\left(\frac{\partial \boldsymbol{g}_i}{\partial \boldsymbol{\theta}_i^n} \right)^T \left(\frac{\partial \boldsymbol{g}_i}{\partial \boldsymbol{\theta}_i^n} \right) \right]^{-1} \left(\frac{\partial \boldsymbol{g}_i}{\partial \boldsymbol{\theta}_t^n} \right)^T \left[\boldsymbol{g}_i \left(\boldsymbol{\theta}^n, \ddot{x}_g \right) - \ddot{\boldsymbol{x}}_{mea,i} \right] \tag{22}$$

$$\left(i = 1, 2 \cdots r \right)$$

When an iterative SOR method is used to solve Eq. (5) for each Newton iteration, the entire process is called the Newton-SOR method (Ortega and Rheinboldt 1970). If p iterations are used within the SOR loop, then the method is called *p-step* Newton-SOR. Comprehensive descriptions of the method were discussed by Ortega and Rheinboldt (1970). The SOR solution is used to reconstruct the Jacobian matrix for the succeeding Newton step such that the SOR solution is not required to have high precision (Law *et al*. 2014, Ni *et al*. 2018). Therefore, we only consider the one-step Newton-SOR method. The Jacobian matrix or dynamic response sensitivity is calculated in the next section.

2.3 Dynamic response sensitivity considering material nonlinearity

Structural response sensitivity has been studied for years and extensively used for probabilistic analysis, structural design optimisation and reliability analysis (Conte 2001, Haukaas and Der Kiureghian 2004, Ye *et al*. 2015). Numerous methods, such as finite difference (Hsieh and Arora 1984), perturbation (Kiran *et al.* 2016), direct differentiation (Gu *et al*. 2009) and substructuring methods, have been proposed to calculate sensitivity. Although the perturbation method is computationally efficient, it may not be accurate enough. The forward finite difference method is simple, but it is time consuming and vulnerable to numerical errors. The direct differentiation method trades off accuracy and computational efficiency and has been extensively used in nonlinear FE model updating (Astroza *et al*. 2014, Ebrahimian *et al*. 2015, Ebrahimian *et al.* 2017). Therefore, this method is adopted in this study and briefed as follows.

The acceleration and velocity at time step (t+1) can be interpolated with an implicit time integration scheme as follows

$$\ddot{\boldsymbol{x}}(t+1) = b_1 \boldsymbol{x}(t+1) + b_2 \boldsymbol{x}(t) + b_3 \dot{\boldsymbol{x}}(t) + b_4 \ddot{\boldsymbol{x}}(t) \tag{23}$$

$$\dot{\boldsymbol{x}}(t+1) = b_5 \boldsymbol{x}(t+1) + b_6 \boldsymbol{x}(t) + b_7 \dot{\boldsymbol{x}}(t) + b_8 \ddot{\boldsymbol{x}}(t) \tag{24}$$

where b_1 to b_8 are constant integration coefficients. By substituting Eqs. (23) and (24) into Eq. (1), we have

$$b_1 \boldsymbol{M} \boldsymbol{x}(t+1) + b_5 \boldsymbol{C} \boldsymbol{x}(t+1) + \boldsymbol{K}_r \left(\boldsymbol{x}(t+1), \boldsymbol{\theta} \right) = \boldsymbol{P}(t+1) \tag{25}$$

where

$$\begin{aligned} \boldsymbol{P}(t+1) = {} & \boldsymbol{MI}\ddot{x}_g (t+1) - \boldsymbol{M} \left[b_2 \boldsymbol{x}(t) + b_3 \dot{\boldsymbol{x}}(t) + b_4 \ddot{\boldsymbol{x}}(t) \right] \\ & - \boldsymbol{C} \left[b_6 \boldsymbol{x}(t) + b_7 \dot{\boldsymbol{x}}(t) + b_8 \ddot{\boldsymbol{x}}(t) \right] \end{aligned} \tag{26}$$

Eq. (25) is differentiated with respect to each material parameter θ_i to obtain the response sensitivity as follows

$$\begin{aligned} & \left[b_1 \boldsymbol{M} \boldsymbol{x}(t+1) + b_5 \boldsymbol{C} \boldsymbol{x}(t+1) + \frac{\partial \boldsymbol{K}_r \left(\boldsymbol{x}(t+1), \boldsymbol{\theta} \right)}{\partial \boldsymbol{x}(t+1)} \right] \frac{\partial \boldsymbol{x}(t+1)}{\partial \theta_i} \\ & = - \frac{\partial \boldsymbol{K} \left(\boldsymbol{x}(t+1), \boldsymbol{\theta} \right)}{\partial \theta_i} + \frac{\partial \boldsymbol{P}(t+1)}{\partial \theta_i} - \left(b_1 \frac{\partial \boldsymbol{M}}{\partial \theta_i} + b_5 \frac{\partial \boldsymbol{C}}{\partial \theta_i} \right) \boldsymbol{x}(t+1) \end{aligned} \tag{27}$$

This study only considers nonlinear material parameters in the material constitutive model. Therefore, $\partial \boldsymbol{M} / \partial \theta_i = 0$ and $\partial \boldsymbol{C} / \partial \theta_i = 0$. The last term on the right-hand side of Eq. (27) can be negligible. Similarly, by using the derivative of Eq. (26) with respect to θ_i, we have

$$\begin{aligned} \frac{\partial \boldsymbol{P}(t+1)}{\partial \theta_i} = {} & \frac{\partial \boldsymbol{MI}\ddot{x}_g (t+1)}{\partial \theta_i} - \frac{\partial \boldsymbol{M}}{\partial \theta_i} \left[b_2 \boldsymbol{x}(t) + b_3 \dot{\boldsymbol{x}}(t) + b_4 \ddot{\boldsymbol{x}}(t) \right] - \frac{\partial \boldsymbol{C}}{\partial \theta_i} \left[b_6 \boldsymbol{x}(t) + b_7 \dot{\boldsymbol{x}}(t) + b_8 \ddot{\boldsymbol{x}}(t) \right] \\ & - \boldsymbol{M} \left[b_2 \frac{\partial \boldsymbol{x}}{\partial \theta_i}(t) + b_3 \frac{\partial \dot{\boldsymbol{x}}}{\partial \theta_i}(t) + b_4 \frac{\partial \ddot{\boldsymbol{x}}}{\partial \theta_i}(t) \right] - \boldsymbol{C} \left[b_6 \frac{\partial \boldsymbol{x}}{\partial \theta_i}(t) + b_7 \frac{\partial \dot{\boldsymbol{x}}}{\partial \theta_i}(t) + b_8 \frac{\partial \ddot{\boldsymbol{x}}}{\partial \theta_i}(t) \right] \\ = {} & - \boldsymbol{M} \left[b_2 \frac{\partial \boldsymbol{x}}{\partial \theta_i}(t) + b_3 \frac{\partial \dot{\boldsymbol{x}}}{\partial \theta_i}(t) + b_4 \frac{\partial \ddot{\boldsymbol{x}}}{\partial \theta_i}(t) \right] - \boldsymbol{C} \left[b_6 \frac{\partial \boldsymbol{x}}{\partial \theta_i}(t) + b_7 \frac{\partial \dot{\boldsymbol{x}}}{\partial \theta_i}(t) + b_8 \frac{\partial \ddot{\boldsymbol{x}}}{\partial \theta_i}(t) \right] \end{aligned} \tag{28}$$

Vectors $\partial \boldsymbol{x}(t) / \partial \theta_i$, $\partial \dot{\boldsymbol{x}}(t) / \partial \theta_i$ and $\partial \ddot{\boldsymbol{x}}(t) / \partial \theta_i$ are available from the last time step sensitivity computation. Therefore, $\partial \boldsymbol{P}(t+1) / \partial \theta_i$ can be obtained. The first term in the right-hand side of Eq. (27), that is, $\partial \boldsymbol{K}_r \left(\boldsymbol{x}(t+1), \boldsymbol{\theta} \right) / \partial \theta_i$, is the partial derivative of the resisting force with respect to the unknown material parameter θ_i. The internal resisting force vector $\boldsymbol{K}_r \left(\boldsymbol{x}(t+1), \boldsymbol{\theta} \right)$ can be assembled from the element nodal resisting force as follows

$$\boldsymbol{K}_r \left(\boldsymbol{x}(t+1), \boldsymbol{\theta} \right) = \sum_{i=1}^{ne} \left\{ K_{t+1}^{ele,i} \left(\boldsymbol{x}_i (t+1), \boldsymbol{\theta} \right) \right\} \tag{29}$$

where $\boldsymbol{x}_i (t+1)$ is the element nodal displacement vector in the element local coordinate system, ne denotes the total number of elements and $K_{t+1}^{ele,i}$ represents the ith element nodal resisting force vector at time step (t+1) and is obtained from the integral of the section stress vector as follows

$$K_{t+1}^{ele,i} = \int \boldsymbol{B}^T \boldsymbol{\sigma}_{t+1}^{\sec} \left(\boldsymbol{\varepsilon}_{t+1}^{\sec} (\boldsymbol{\theta}), \boldsymbol{\theta} \right) dl \tag{30}$$

where $\boldsymbol{B}$ indicates the strain-displacement transformation matrix, $\boldsymbol{\varepsilon}_{t+1}^{sec}$ refers to the section strain and $\boldsymbol{\sigma}_{t+1}^{sec}$ is the section stress vector that is obtained by integrating the fibre stresses over the cross section as follows

$$\boldsymbol{\sigma}_{t+1}^{sec} = \int \boldsymbol{b} \sigma_{t+1}^{fib} \left(\varepsilon_{t+1}^{fib} (\boldsymbol{\theta}), \boldsymbol{\theta} \right) dA \tag{31}$$

where b is the section kinematic vector; σ_{t+1}^{fib} represents the fibre stress; and ε_{t+1}^{fib} denotes the fibre strain.

By substituting Eqs. (30) and (31) into Eq. (29), the partial derivative is computed as follows

$$\frac{\partial \boldsymbol{K}_r \left(\boldsymbol{x}(t+1), \boldsymbol{\theta} \right)}{\partial \theta_i} = \sum_{i=1}^{ne} \left\{ \int \boldsymbol{B}^T \int \boldsymbol{b} \frac{\partial \sigma_{t+1}^{fib} \left(\varepsilon_{t+1}^{fib} (\boldsymbol{\theta}), \boldsymbol{\theta} \right)}{\partial \theta_i} dA dl \right\} \tag{32}$$

where $\partial\sigma_{t+1}^{fib}\left(\varepsilon_{t+1}^{fib}(\boldsymbol{\theta}),\boldsymbol{\theta}\right)/\partial\theta_i$ is the derivative of the fibre stress with respect to material parameter θ_i and can be computed by analytically differentiating the material constitutive law (Zhang and Der Kiureghian 1993, Kleiber *et al*. 1997, Conte *et al.* 2003).

2.4 Procedures of the model updating technique

The proposed method is implemented in MATLAB and interfaced with OpenSees (McKenna 2011) for calculating the structural responses and response sensitivity. The procedures of the proposed method are as follows.

Step 1: The structure is divided into small zones on the basis of its FE formulation, and the corresponding sets of responses from each zone are obtained.

Step 2: The initial value of the parameters is set as $\boldsymbol{\theta}=\left[\boldsymbol{\theta}_1^0,\boldsymbol{\theta}_2^0,\cdots,\boldsymbol{\theta}_r^0\right]$.

Step 3: The sensitivity of responses is computed with respect to the structural parameters of each zone with OpenSees.

Step 4: The parameters of each zone $\boldsymbol{\theta}_i^{n+1}$ are updated using Eq. (22).

Step 5: Steps 3-4 are repeated until the following convergence criterion in Eq. (33) is satisfied.

$$\frac{\left\|\boldsymbol{\theta}^{n+1}-\boldsymbol{\theta}^{n}\right\|}{\left\|\boldsymbol{\theta}^{n+1}\right\|}\times 100\% \le Tol \tag{33}$$

where *Tol* is the tolerance of convergence criterion, which is set as 1.0×10^{-8} and 1.0×10^{-5} for cases without and with noise, respectively, in following examples.

3. Numerical examples

3.1 RC frame

A two-bay, three-floor RC planar frame structure is studied. Fig. 2(a) shows the dimensions of the frame model. Each bay of the structure has a length of 5 m and the height of each floor is 3 m. The cross sections of columns and beams are 0.5 m×0.5 m and 0.25 m×0.4 m, respectively (Figs. 2(b-c)). This structure is modeled with displacement-based fiber-section beam-column elements in OpenSees. The columns and beams on each floor are further divided into 5 and 10 elements, respectively, along the longitudinal direction. Therefore, the FE model of the structure comprises 102 nodes, 105 elements and 306 DOFs, as shown in Fig. 3. The beam and column sections are discretized into several fibers, as shown in Fig. 4. The longitudinal reinforcement is modelled with the uniaxial Menegotto-Pinto steel material (Barbato and Conte 2006). The concrete is modeled with the uniaxial smoothed Popovics-Saenz concrete material (Zona *et al*. 2005). Figs. 5(a-f) show the stress–strain relations and hysteresis curves of the steel and concrete. Table 1 lists the material parameters of the longitudinal reinforcement, confined concrete and unconfined concrete. These parameters are selected from previous studies (Zona *et al.* 2005, Gu *et al.* 2009).

The El Centro earthquake with a peak ground acceleration (PGA) of 0.8 g is selected as the input. The nonlinear dynamic responses of the structure are computed using the Newmark method. A mass of 4,000 kg/m is added to the beam elements to simulate the weight of floors and other dead loads. As shown in Fig. 5, the entire structure is divided into three zones. Three accelerometers are installed in each zone to measure the horizontal acceleration responses. The sampling frequency is 1000 Hz and the ground motion lasts for 20 s. The measured responses in each zone are used to update the material parameters of that zone.

Table 1 Material parameters of the RC frame structure

Material	Unknown material parameters (initial values)
Confined concrete	Compressive strength f_c (34.5 MPa) Concrete strain at maximum strength ε_c (0.005) Initial tangent stiffness E_c (27.9 GPa)
Unconfined concrete	Compressive strength f_{uc} (27.6 MPa) Concrete strain at maximum strength ε_{uc} (0.002) Initial tangent stiffness E_{uc} (24.9 GPa)
Reinforcement	Initial yield stress f_y (248.2 MPa) Young's modulus E_s (210 GPa) Strain-hardening ratio b (0.02)

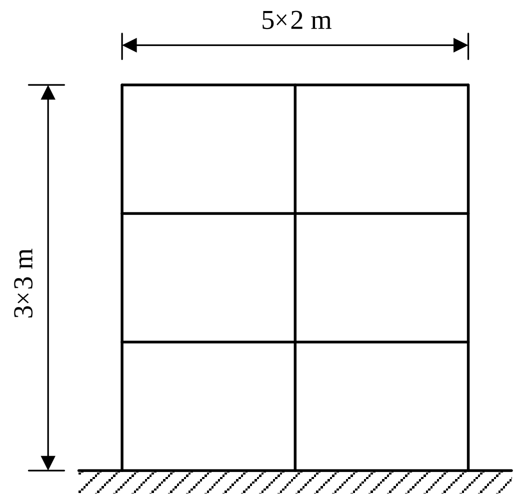

(a) Frame structure

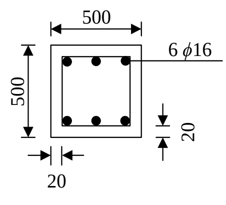

(b) Column (unit: mm)

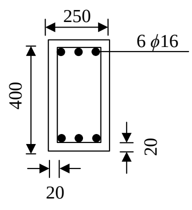

(c) Beam (unit: mm)

Fig. 2 Dimensions of RC frame structure

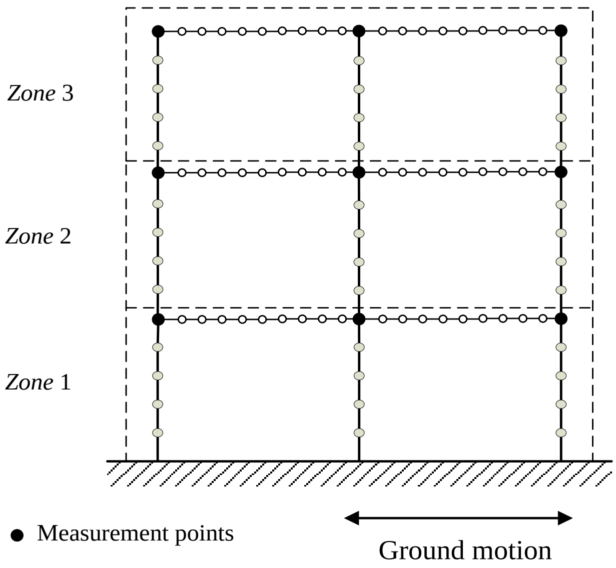

Fig. 3 FE model of frame structure

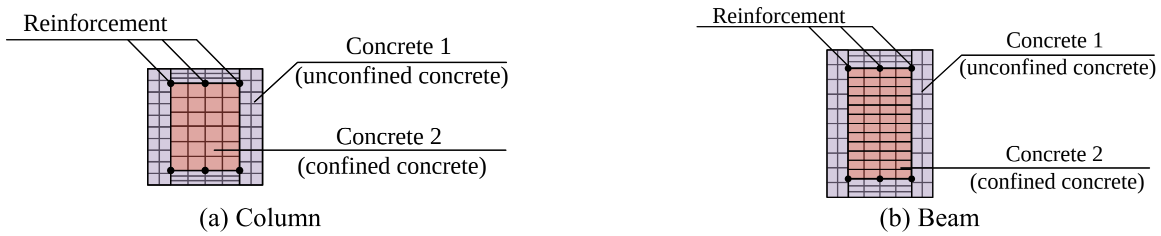

(a) Column (b) Beam

Fig. 4 Fibers defined in the cross section

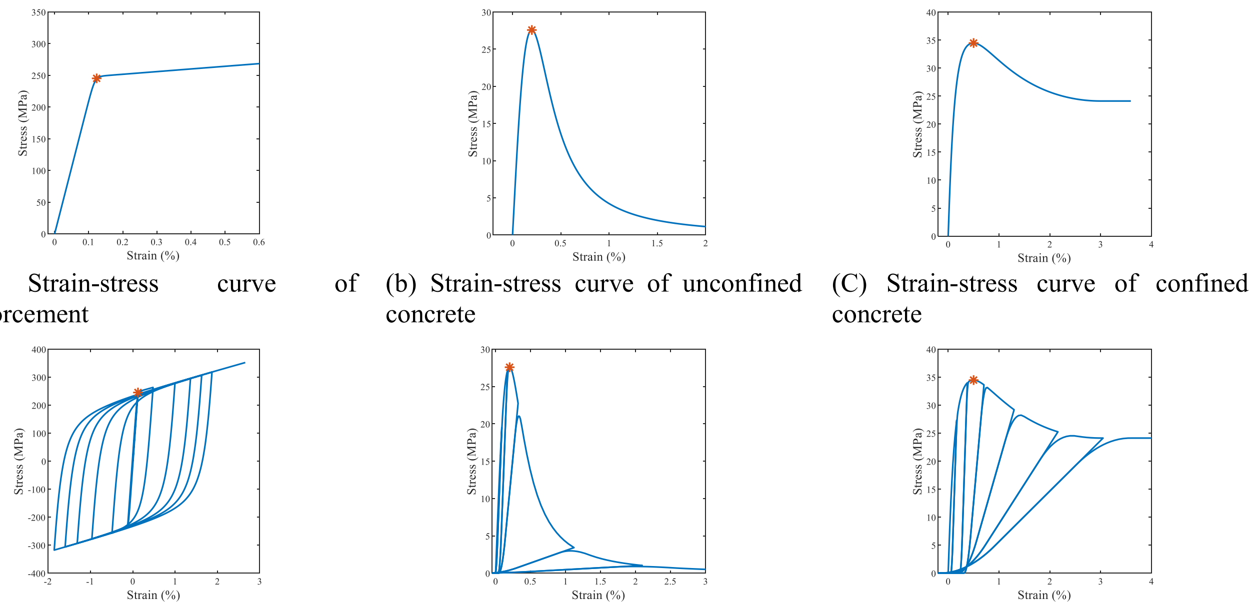

(a) Strain-stress curve of reinforcement

(b) Strain-stress curve of unconfined concrete

(C) Strain-stress curve of confined concrete

(d) Hysteresis loop of reinforcement

(e) Hysteresis loop of unconfined concrete

(f) Hysteresis loop of confined concrete

Fig. 5 Material models

Material parameters in the constitutive model for each floor are the same. The unknown variables are compressive strength f_c, concrete strain at maximum strength ε_c, initial tangent stiffness of the confined concrete E_c, compressive strength f_{uc}, concrete strain at maximum strength ε_{uc}, initial tangent stiffness of the unconfined concrete E_{uc}, initial yield stress f_y, Young's modulus E_s and strain-hardening ratio of reinforcement b. Other empirical parameters that control the curvature of the hysteretic loops are assumed as known constants. Therefore, each zone has 9 unknown material parameters and the entire structure has 27 to be identified. Table 1 lists the initial values of the material parameters. To simulate the uncertainty in the material parameters, 10% random errors are added to such parameters.

With the measured acceleration responses, the material parameters in each zone are identified using the proposed decentralized approach. Fig. 6 shows the results with a comparison of the true values. The identified material parameters in each zone are consistent with the true values, thereby verifying the accuracy of the proposed method. Fig. 7 compares the computational time and relative errors between the proposed decentralized and conventional global model updating methods. The latter is based on the classic sensitivity-based model updating method (Lu and Law 2007). The decentralized method converges to the true values in approximately 3.5 h; it is considerably faster than the global method, which takes 11 h.

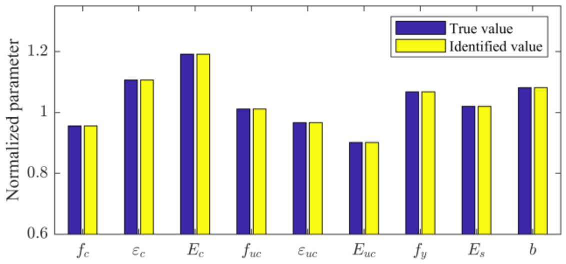

(a) Subset 1

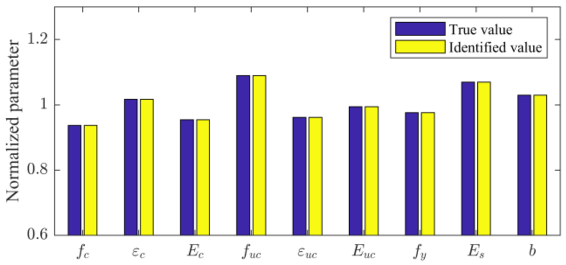

(b) Subset 2

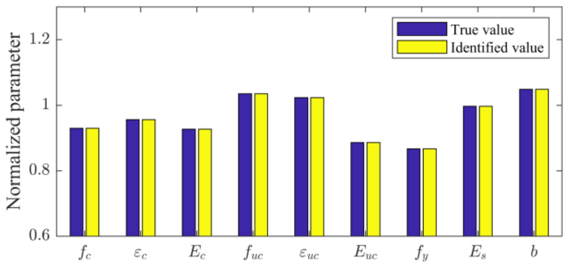

(c) Subset 3

Fig. 6 Identified parameters of the RC structure

The effect of measurement noise on the identified results is considered, in which 5% and 10% measurement noises are evaluated. A random noise is added to the actual responses as

$$\ddot{x}_{mea} = \ddot{x} + E_p N_{noise} \sigma(\ddot{x}) \tag{34}$$

where E_p is the percentage of the noise level; N_{noise} denotes a standard normal distribution vector with a zero mean and unit standard deviation; and $\sigma(\ddot{x})$ indicates the standard deviation of the actual acceleration response.

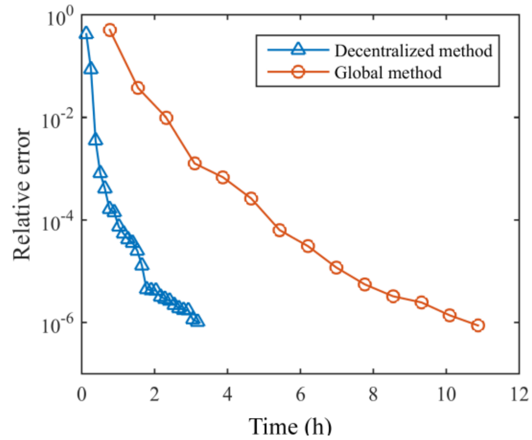

Fig. 7 Computational time of the decentralized and global methods

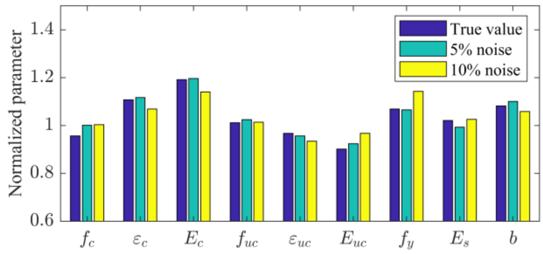

(a) Subset 1

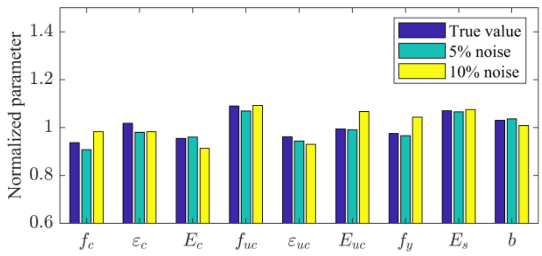

(b) Subset 2

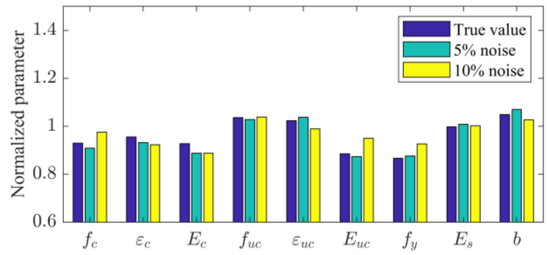

(c) Subset 3

Fig. 8 Identified parameters using noisy measurement data

Fig. 8 shows the identified normalised parameters of each subset with different noise levels. The error generally increases as the noise level increases. When 5% measurement noise is added, the large identification errors are 3.64% (f_c in Subset 1), 4.45% (ε_c in Subset 2) and 4.21% (E_c in Subset 3). The other errors are relatively small. In the case of 10% measurement noise, the large errors are 7.26% (E_{uc} in Subset 1), 5.72% (b in Subset 2) and 6.48% (ε_{uc} in Subset 3). The identification errors are acceptable in both cases.

3.2 Steel frame

A one-bay, six-floor steel planar frame structure is investigated. Fig. 9(a) shows the dimensions of the frame structure model. The height of each floor is 3.5 m, and the building width is 6 m. The beams of the frame are composed of W14×61 wide flange beams, and the columns of each floor have the same section with a width of 400 mm and thickness of 8 mm. Figs. 9(b) and (c) shows the cross sections of the columns and beams, respectively. The beams and columns are welded to form rigid joints. The bottom of the frame is fixed on the strong floor. The columns and beams on each floor are further divided into five elements.

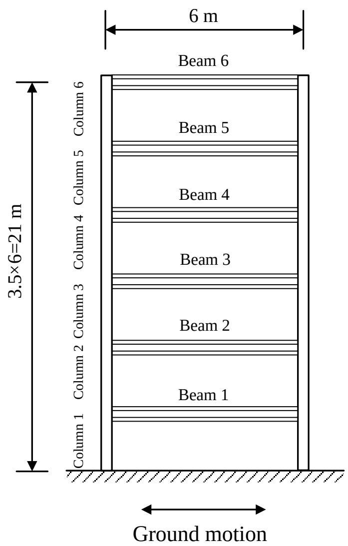

(a) Steel frame structure

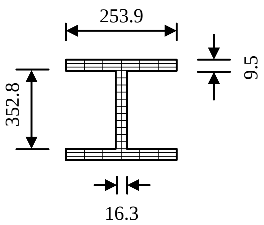

(b) Cross section of beam (unit: mm)

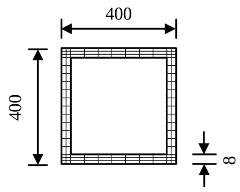

(c) Cross section of column (unit: mm)

Fig. 9 Dimensions of steel structure

Table 2 Material parameters of steel structure

Member	Initial yield stress (f_y, MPa)	Young's modulus (E_s, GPa)	Strain-hardening ratio
Columns 1-2 Beams 1-2	350	210	0.02
Columns 3-4 Beams 3-4	300	210	0.02
Columns 5-6 Beams 5-6	200	210	0.02

The structural elements are modeled with displacement-based, fiber-section and beam–column elements. Therefore, the FE model of the structure comprises 86 nodes, 90 elements and 258 DOFs. The constitutive behavior of the steel material is simulated with the uniaxial Menegotto-Pinto steel material (Barbato and Conte 2006). In each floor, initial yield stress f_y and Young's modulus E_s in the constitutive model of the columns and beams are set as unknown variables, resulting in a total of 6×4 unknown material parameters to be identified. Table 2 lists the initial material parameters used in this example. A 10% model error is considered in the material parameters.

The dynamic responses of the building under the El Centro earthquake (PGA = 0.8 g) are computed on the basis of the nonlinear FE model. Six accelerometers are installed at the beam and column joints for measuring the horizontal acceleration responses at the sampling frequency of 1,000 Hz. The structure is divided into two zones.

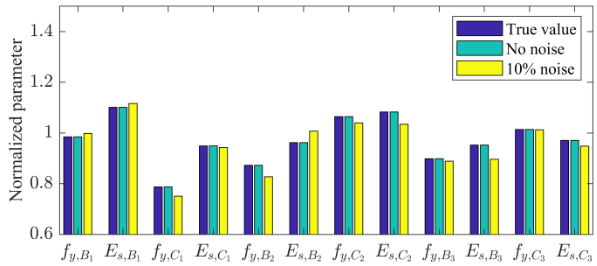

(a) Subset 1

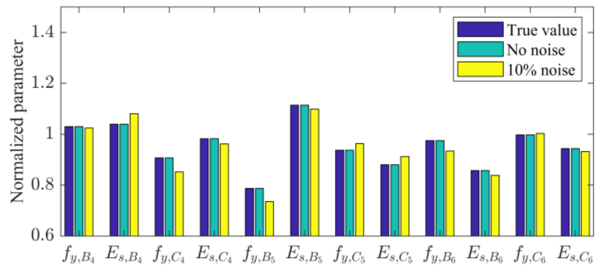

(b) Subset 2

Fig. 10 Normalized identified results of the steel structure ($f_{y,\,Bi}$ and $f_{y,\,Ci}$ denote the yield stress of the beam and column at the ith floor, respectively; $E_{s,\,Bi}$ and $E_{s,\,Ci}$ represent the Young's modulus of the beam and column at the ith floor, respectively)

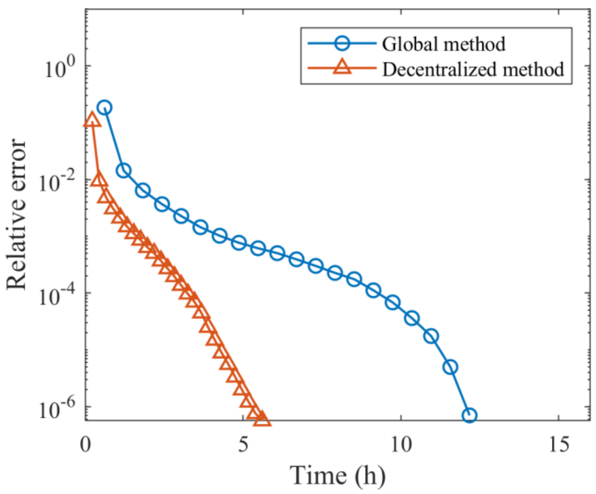

Fig. 11 Computational time of steel structure with global and decentralized methods

The first zone contains the acceleration responses from the first to third floors, whereas the second zone contains those of the fourth to sixth floors. Each subset of responses is used to update the corresponding material parameters in the same zone, in which the first 50 s vibration responses are used.

Fig. 10 shows the model updating results based on the measurement data. The accuracy of the proposed decentralized model updating method is likewise verified. The identified normalized parameters, without considering measurement noise, remarkably match their true values. When 10% noise is added to the actual responses, the largest identification error is 5.72% ($E_{s,\,B3}$) in Subset 1 and 5.49% ($f_{y,\,C4}$) in Subset 2. Fig. 11 compares the proposed decentralized and global methods in terms of the identification errors and computational time. The decentralized and global methods take 6 and 12 h, respectively, to achieve the same level of precision. These results demonstrate the accuracy and robustness of the proposed method.

4. Conclusions

A decentralized model updating technique is proposed to identify the structural nonlinear parameters under earthquake excitations. In comparison with the global model updating technique, the decentralized approach divides a global structure into several zones. Then, the unknown nonlinear material parameters in each zone are updated using the vibration measurements of the same zone via a one-step Newton-SOR method. The nonlinear dynamic responses of the structure are calculated using a fiber element model. The sensitivity of the dynamic responses with respect to the material parameters is derived using the direct difference method. The proposed method is applied to two numerical structures subjected to seismic inputs. Results show that nonlinear parameters in the material constitutive model, such as the compressive strength, concrete strain at maximum strength and initial tangent stiffness, can be identified with high accuracy even when 10% measurement noise is included. Comparative studies with the global model updating technique demonstrate that the proposed method can identify unknown material parameters with less computational time.

Acknowledgments

The work described in this paper was jointly supported by the National Science Foundation of China (Grant Nos. 51822810 and 51778574), the Zhejiang Provincial Natural Science Foundation of China (Grant No. LR19E080002), and the Fundamental Research Funds for the Central Universities of China (Grant No. 2019XZZX004-01).

References

Asgarieh, E., Moaveni, B. and Stavridis, A. (2014), "Nonlinear finite element model updating of an infilled frame based on identified time-varying modal parameters during an earthquake", *J. Sound. Vib.*, **333**(23), 6057-6073. DOI:10.1016/j.jsv.2014.04.064.

Astroza, R., Ebrahimian, H. and Conte, J.P. (2014), "Material parameter identification in distributed plasticity FE models of frame-type structures using nonlinear stochastic filtering", *J. Eng. Mech.*, **141**(5), 04014149. DOI:10.1061/(ASCE)EM.1943-7889.0000851.

Astroza, R., Ebrahimian, H., Li, Y. and Conte, J.P. (2017), "Bayesian nonlinear structural FE model and seismic input identification for damage assessment of civil structures", *Mech. Syst. Signal. Pr.*, **93**, 661-687. DOI:10.1016/j.ymssp.2017.01.040.

Barbato, M. and Conte, J.P. (2006), "Finite element structural response sensitivity and reliability analyses using smooth versus non-smooth material constitutive models", *Inter. J. Reliab. Safe.*, **1**(1-2), 3-39. DOI: 10.1504/IJRS.2006.010688.

Conte, J.P. (2001), "Finite element response sensitivity analysis in earthquake engineering", Earthquake Engineering Frontiers in the New Millennium, pp.395-401.

Conte, J., Vijalapura, P. and Meghella, M. (2003), "Consistent finite-element response sensitivity analysis", *J. Eng. Mech.*, **129**(12), 1380-1393. DOI: 10.1061/(ASCE)0733-9399(2003)129:12(1380).

Chen, G., Yang, X., Ying, X. and Nanni, A. (2006), "Damage detection of concrete beams using nonlinear features of forced vibration", *Struct. Health. Monit.*, **5**(2), 125-141. DOI: 10.1177/1475921706057985.

Charalampakis, A. and Koumousis, V. (2008), "Identification of Bouc-Wen hysteretic systems by a hybrid evolutionary algorithm", *J. Sound. Vib.*, **314**(3), 571-585. DOI: 10.1016/j.jsv.2008.01.018.

Chatzi, E.N. and Smyth, A.W. (2009), "The unscented Kalman filter and particle filter methods for nonlinear structural system identification with non-collocated heterogeneous sensing", *Struct. Control. Health.*, **16**(1), 99-123. DOI: 10.1002/stc.290.

Ebrahimian, H., Astroza, R. and Conte, J.P. (2015), "Extended Kalman filter for material parameter estimation in nonlinear structural finite element models using direct differentiation method", *Earthq. Eng. Struct.*, **44**(10), 1495-1522. DOI: 10.1002/eqe.2532.

Ebrahimian, H., Astroza, R., Conte, J.P. and de Callafon, R.A. (2017), "Nonlinear finite element model updating for damage identification of civil structures using batch Bayesian estimation", *Mech. Syst. Signal. Pr.*, **84**, 194-222. DOI: 10.1016/j.ymssp.2016.02.002.

Ebrahimian, H., Astroza, R., Conte, J.P. and Papadimitriou, C. (2018), "Bayesian optimal estimation for output-only nonlinear system and damage identification of civil structures", *Struct. Control. Health.*, **25**(4), e2128. DOI: 10.1002/stc.2128.

Friswell, M. and Mottershead, J.E. (2013), Finite Element Model Updating in Structural Dynamics., Springer Science & Business Media.

Gu, Q., Conte, J.P., Elgamal, A. and Yang, Z. (2009), "Finite element response sensitivity analysis of multi-yield-surface J2 plasticity model by direct differentiation method", *Comput. Method Appl. M.*, **198**(30-32), 2272-2285. DOI: 10.1016/j.cma.2009.02.030.

Hsieh, C. and Arora, J. (1984), "Design sensitivity analysis and optimization of dynamic response", *Comput. Method Appl. M.*, **43**(2), 195-219. DOI: 10.1016/0045-7825(84)90005-7.

Haukaas, T. and Der Kiureghian, A. (2004), Finite Element Reliability and Sensitivity Methods for Performance-based Earthquake Engineering, Pacific Earthquake Engineering Research Center, College of Engineering, University of California, Berkeley.

He, J., Xu, B. and Masri, S.F. (2012), "Restoring force and dynamic loadings identification for a nonlinear chain-like structure with partially unknown excitations", *Nonlinear Dynam.*, **69**(1-2), 231-245. DOI: 10.1007/s11071-011-0260-7.

Kleiber, M., Tran, D.H., Antùnez, H. and Kowalczyk, P. (1997), Parameter Sensitivity in Nonlinear Mechanics: Theory and Finite Element Computations., John Wiley, Chichester, England.

Kim, J. and Lynch, J.P. (2011), "Autonomous decentralized system identification by Markov parameter estimation using distributed smart wireless sensor networks", *J. Eng. Mech.*, **138**(5), 478-490. DOI: 10.1061/(ASCE)EM.1943-7889.0000359.

Kiran, R., Li, L. and Khandelwal, K. (2016), "Complex perturbation method for sensitivity analysis of nonlinear trusses", *J. Struct. Eng.*, **143**(1), 04016154. DOI: 10.1061/(ASCE)ST.1943-541X.0001619.

Lei, Y. and Wu, Y. (2011). "Non-parametric identification of structural nonlinearity with limited input and output measurements", *Adv. Mater. Res.*, **243**: 5403-5407. DOI: 10.4028/www.scientific.net/AMR.243-249.5403.

Lei, Y., Wu, D. and Liu, L. (2013), "A decentralized structural control algorithm with application to the benchmark control problem for seismically excited buildings", *Struct. Control. Health.*, **20**(9), 1211-1225. DOI: 10.1002/stc.1529.

Law, S.S., Ni, P.H. and Li, J. (2014), "Parallel decentralized damage detection of a structure with subsets of parameters", *AIAA. J.*, **52**(3), 650-656. DOI: 10.2514/1.J051716.

Li, Y., Astroza, R., Conte, J.P. and Soto, P. (2017), "Nonlinear FE model updating and reconstruction of the response of an instrumented seismic isolated bridge to the 2010 Maule Chile earthquake", *Earthq. Eng. Struct.*, **46**(15), 2699-2716. DOI: 10.1002/eqe.2925.

Lu, Z.R. and Law, S.S. (2007), "Features of dynamic response sensitivity and its application in damage detection", *J. Sound. Vib.*, **303**(1-2), 305-329. DOI: 10.1016/j.jsv.2007.01.021.

McKenna, F. (2011), "OpenSees: a framework for earthquake engineering simulation", *Comput. Sci. Eng.*, **13**(4), 58-66. DOI: 10.1109/MCSE.2011.66.

Ni, P., Xia, Y., Law, S. S. and Zhu, S. (2014), "Structural damage detection using auto/cross-correlation functions under multiple unknown excitations", *Int. J. Struct. Stab. Dy.*, **14**(5). DOI: 10.1142/S0219455414400069.

Ni, P., Xia, Y., Li, J. and Hao, H. (2018), "Improved decentralized structural identification with output-only measurements", *Measurement*, **122**, 597-610. DOI: 10.1016/j.measurement.2017.09.029.

Ortega, J.M. and Rheinboldt, W.C. (1970), Iterative Solution of Nonlinear Equations in Several Variables., SIAM. DOI: 10.1016/C2013-0-11263-9.

Prawin, J., Rao, A. and Mohan, R. (2018), "Detection of nonlinear structural behavior using time-frequency and multivariate analysis", *Smart Struct. Syst.*, **22**(6), 711-725. https://doi.org/10.12989/sss.2018.22.6.711.

Smyth, A., Masri, S., Chassiakos, A. and Caughey, T. (1999), "On-line parametric identification of MDOF nonlinear hysteretic systems", *J. Eng. Mech.*, **125**(2), 133-142. DOI: 10.1061/(ASCE)0733-9399(1999)125:2(133).

Taucer, F., Spacone, E. and Filippou, F.C. (1991), A Fiber Beam-Column Element for Seismic Response Analysis of Reinforced Concrete Structures., Berkekey, California: Earthquake Engineering Research Center, College of Engineering, University of California.

Ting, J.A., Mistry, M., Peters, J., Schaal, S. and Nakanishi, J. (2006), "A Bayesian approach to nonlinear parameter identification for rigid body dynamics", In Robotics: Science and Systems (pp. 32-39). DOI: 10.15607/RSS.2006.II.032.

Xu, B., Wu, Z. and Yokoyama, K. (2003), "Neural networks for decentralized control of cable-stayed bridge", J. *Bridge Eng.*, **8**(4), 229-236. DOI: 10.1061/(ASCE)1084-0702(2003)8:4(229).

Xu, B., He, J. and Masri, S.F. (2012), "Data-based identification of nonlinear restoring force under spatially incomplete excitations with power series polynomial model", *Nonlinear Dynam.*, **67**(3), 2063-2080. DOI: 10.1007/s11071-011-0129-9.

Yuen, K.V. and Beck, J.L. (2003), "Updating properties of nonlinear dynamical systems with uncertain input", *J. Eng. Mech.*, **129**(1), 9-20. DOI:10.1061/(ASCE)0733-9399(2003)129:1(9).

Ye, X.W., Ni, Y.Q., Wai, T.T., Wong, K.Y., Zhang, X.M. and Xu, F. (2013), "A vision-based system for dynamic displacement measurement of long-span bridges: algorithm and verification", *Smart Struct Syst.*, **12**(3-4), 363-379. https://doi.org/10.12989/sss.2013.12.3_4.363.

Ye, X.W., Yi, T.H., Wen, C. and Su, Y.H. (2015), "Reliability-based assessment of steel bridge deck using a mesh-insensitive structural stress method", *Smart Struct Syst.*, **16**(2), 367-382. https://doi.org/10.12989/sss.2015.16.2.367.

Ye, X.W., Dong, C.Z. and Liu, T. (2016a), "Force monitoring of steel cables using vision-based sensing technology: methodology and experimental verification", *Smart Struct Syst.*, **18**(3), 585-599. https://doi.org/10.12989/sss.2016.18.3.585.

Ye, X.W., Dong, C.Z. and Liu, T. (2016b), "Image-based structural dynamic displacement measurement using different multi-object tracking algorithms", *Smart Struct Syst.*, **17**(6), 935-956. https://doi.org/10.12989/sss.2016.17.6.935.

Zhang, Y. and Der Kiureghian, A. (1993), "Dynamic response sensitivity of inelastic structures", *Comput. Method Appl. M.*, **108**(1), 23-36. DOI:10.1016/0045-7825(93)90151-M.

Zona, A., Barbato, M. and Conte, J.P. (2005), "Finite element response sensitivity analysis of steel-concrete composite beams with deformable shear connection", *J. Eng. Mech.*, **131**(11), 1126-1139. DOI: 10.1061/(ASCE)0733-9399(2005)131:11(1126).